

UC Irvine

UC Irvine Previously Published Works

Title

Observation of a Neutral Structure near the DD^* Mass Threshold in $e^+e^- \rightarrow (DD^*)0\pi^0$ at $s=4.226$ and 4.257 GeV

Permalink

<https://escholarship.org/uc/item/6355174t>

Journal

Physical Review Letters, 115(22)

ISSN

0031-9007

Authors

Ablikim, M

Achasov, MN

Ai, XC

et al.

Publication Date

2015-11-27

DOI

10.1103/physrevlett.115.222002

Copyright Information

This work is made available under the terms of a Creative Commons Attribution License, available at <https://creativecommons.org/licenses/by/4.0/>

Peer reviewed

Observation of a Neutral Structure near the $D\bar{D}^*$ Mass Threshold in $e^+e^- \rightarrow (D\bar{D}^*)^0\pi^0$ at $\sqrt{s} = 4.226$ and 4.257 GeV

M. Ablikim¹, M. N. Achasov^{9,f}, X. C. Ai¹, O. Albayrak⁵, M. Albrecht⁴, D. J. Ambrose⁴⁴, A. Amoroso^{49A,49C}, F. F. An¹, Q. An^{46,a}, J. Z. Bai¹, R. Baldini Ferroli^{20A}, Y. Ban³¹, D. W. Bennett¹⁹, J. V. Bennett⁵, M. Bertani^{20A}, D. Bettini^{21A}, J. M. Bian⁴³, F. Bianchi^{49A,49C}, E. Boger^{23,d}, I. Boyko²³, R. A. Briere⁵, H. Cai⁵¹, X. Cai^{1,a}, O. Cakir^{40A,b}, A. Calcaterra^{20A}, G. F. Cao¹, S. A. Cetin^{40B}, J. F. Chang^{1,a}, G. Chelkov^{23,d,e}, G. Chen¹, H. S. Chen¹, H. Y. Chen², J. C. Chen¹, M. L. Chen^{1,a}, S. Chen Chen⁴¹, S. J. Chen²⁹, X. Chen^{1,a}, X. R. Chen²⁶, Y. B. Chen^{1,a}, H. P. Cheng¹⁷, X. K. Chu³¹, G. Cibinetto^{21A}, H. L. Dai^{1,a}, J. P. Dai³⁴, A. Dbeyssi¹⁴, D. Dedovich²³, Z. Y. Deng¹, A. Denig²², I. Denysenko²³, M. Destefanis^{49A,49C}, F. De Mori^{49A,49C}, Y. Ding²⁷, C. Dong³⁰, J. Dong^{1,a}, L. Y. Dong¹, M. Y. Dong^{1,a}, S. X. Du⁵³, P. F. Duan¹, J. Z. Fan³⁹, J. Fang^{1,a}, S. S. Fang¹, X. Fang^{46,a}, Y. Fang¹, L. Fava^{49B,49C}, F. Feldbauer²², G. Felici^{20A}, C. Q. Feng^{46,a}, E. Fioravanti^{21A}, M. Fritsch^{14,22}, C. D. Fu¹, Q. Gao¹, X. L. Gao^{46,a}, X. Y. Gao², Y. Gao³⁹, Z. Gao^{46,a}, I. Garzia^{21A}, K. Goetzen¹⁰, W. X. Gong^{1,a}, W. Grad²², M. Greco^{49A,49C}, M. H. Gu^{1,a}, Y. T. Gu¹², Y. H. Guan¹, A. Q. Guo¹, L. B. Guo²⁸, R. P. Guo¹, Y. Guo¹, Y. P. Guo²², Z. Haddadi²⁵, A. Hafner²², S. Han⁵¹, X. Q. Hao¹⁵, F. A. Harris⁴², K. L. He¹, X. Q. He⁴⁵, T. Held⁴, Y. K. Heng^{1,a}, Z. L. Hou¹, C. Hu²⁸, H. M. Hu¹, J. F. Hu^{49A,49C}, T. Hu^{1,a}, Y. Hu¹, G. M. Huang⁶, G. S. Huang^{46,a}, J. S. Huang¹⁵, X. T. Huang³³, Y. Huang²⁹, T. Hussain⁴⁸, Q. Ji¹, Q. P. Ji³⁰, X. B. Ji¹, X. L. Ji^{1,a}, L. W. Jiang⁵¹, X. S. Jiang^{1,a}, X. Y. Jiang³⁰, J. B. Jiao³³, Z. Jiao¹⁷, D. P. Jin^{1,a}, S. Jin¹, T. Johansson⁵⁰, A. Julin⁴³, N. Kalantar-Nayestanaki²⁵, X. L. Kang¹, X. S. Kang³⁰, M. Kavatsyuk²⁵, B. C. Ke⁵, P. Kiese²², R. Kliemt¹⁴, B. Kloss²², O. B. Kolcu^{40B,i}, B. Kopf⁴, M. Kornicer⁴², W. Kühn²⁴, A. Kupsc⁵⁰, J. S. Lange²⁴, M. Lara¹⁹, P. Larin¹⁴, C. Leng^{49C}, C. Li⁵⁰, Cheng Li^{46,a}, D. M. Li⁵³, F. Li^{1,a}, F. Y. Li³¹, G. Li¹, H. B. Li¹, H. J. Li¹, J. C. Li¹, Jin Li³², K. Li³³, K. Li¹³, Lei Li³, P. R. Li⁴¹, T. Li³³, W. D. Li¹, W. G. Li¹, X. L. Li³³, X. M. Li¹², X. N. Li^{1,a}, X. Q. Li³⁰, Z. B. Li³⁸, H. Liang^{46,a}, J. J. Liang¹², Y. F. Liang³⁶, Y. T. Liang²⁴, G. R. Liao¹¹, D. X. Lin¹⁴, B. J. Liu¹, C. X. Liu¹, D. Liu^{46,a}, F. H. Liu³⁵, Fang Liu¹, Feng Liu⁶, H. B. Liu¹², H. H. Liu¹, H. H. Liu¹⁶, H. M. Liu¹, J. Liu¹, J. B. Liu^{46,a}, J. P. Liu⁵¹, J. Y. Liu¹, K. Liu³⁹, K. Y. Liu²⁷, L. D. Liu³¹, P. L. Liu^{1,a}, Q. Liu⁴¹, S. B. Liu^{46,a}, X. Liu²⁶, Y. B. Liu³⁰, Z. A. Liu^{1,a}, Zhiqing Liu²², H. Loehner²⁵, X. C. Lou^{1,a,h}, H. J. Lu¹⁷, J. G. Lu^{1,a}, Y. Lu¹, Y. P. Lu^{1,a}, C. L. Luo²⁸, M. X. Luo⁵², T. Luo⁴², X. L. Luo^{1,a}, X. R. Lyu⁴¹, F. C. Ma²⁷, H. L. Ma¹, L. L. Ma³³, M. M. Ma¹, Q. M. Ma¹, T. Ma¹, X. N. Ma³⁰, X. Y. Ma^{1,a}, F. E. Maas¹⁴, M. Maggiora^{49A,49C}, Y. J. Mao³¹, Z. P. Mao¹, S. Marcello^{49A,49C}, J. G. Messchendorp²⁵, J. Min^{1,a}, R. E. Mitchell¹⁹, X. H. Mo^{1,a}, Y. J. Mo⁶, C. Morales Morales¹⁴, K. Moriya¹⁹, N. Yu. Muchnoi^{9,f}, H. Muramatsu⁴³, Y. Nefedov²³, F. Nerling¹⁴, I. B. Nikolaev^{9,f}, Z. Ning^{1,a}, S. Nisar⁸, S. L. Niu^{1,a}, X. Y. Niu¹, S. L. Olsen³², Q. Ouyang^{1,a}, S. Pacetti^{20B}, Y. Pan^{46,a}, P. Patteri^{20A}, M. Pelizaeus⁴, H. P. Peng^{46,a}, K. Peters¹⁰, J. Pettersson⁵⁰, J. L. Ping²⁸, R. G. Ping¹, R. Poling⁴³, V. Prasad¹, M. Qi²⁹, S. Qian^{1,a}, C. F. Qiao⁴¹, L. Q. Qin³³, N. Qin⁵¹, X. S. Qin¹, Z. H. Qin^{1,a}, J. F. Qiu¹, K. H. Rashid⁴⁸, C. F. Redmer²², M. Ripka²², G. Rong¹, Ch. Rosner¹⁴, X. D. Ruan¹², A. Sarantsev^{23,g}, M. Savrié^{21B}, K. Schoenning⁵⁰, S. Schumann²², W. Shan³¹, M. Shao^{46,a}, C. P. Shen², P. X. Shen³⁰, X. Y. Shen¹, H. Y. Sheng¹, M. Shi¹, W. M. Song¹, X. Y. Song¹, S. Sosio^{49A,49C}, S. Spataro^{49A,49C}, G. X. Sun¹, J. F. Sun¹⁵, S. S. Sun¹, X. H. Sun¹, Y. J. Sun^{46,a}, Y. Z. Sun¹, Z. J. Sun^{1,a}, Z. T. Sun¹⁹, C. J. Tang³⁶, X. Tang¹, I. Tapan^{40C}, E. H. Thorndike⁴⁴, M. Tiemens²⁵, M. Ullrich²⁴, I. Uman^{40B}, G. S. Varner⁴², B. Wang³⁰, D. Wang³¹, D. Y. Wang³¹, K. Wang^{1,a}, L. L. Wang¹, L. S. Wang¹, M. Wang³³, P. Wang¹, P. L. Wang¹, S. G. Wang³¹, W. Wang^{1,a}, W. P. Wang^{46,a}, X. F. Wang³⁹, Y. D. Wang¹⁴, Y. F. Wang^{1,a}, Y. Q. Wang²², Z. Wang^{1,a}, Z. G. Wang^{1,a}, Z. H. Wang^{46,a}, Z. Y. Wang¹, Z. Y. Wang¹, T. Weber²², D. H. Wei¹¹, J. B. Wei³¹, P. Weidenkaff²², S. P. Wen¹, U. Wiedner⁴, M. Wolke⁵⁰, L. H. Wu¹, L. J. Wu¹, Z. Wu^{1,a}, L. Xia^{46,a}, L. G. Xia³⁹, Y. Xia¹⁸, D. Xiao¹, H. Xiao⁴⁷, Z. J. Xiao²⁸, Y. G. Xie^{1,a}, Q. L. Xiu^{1,a}, G. F. Xu¹, J. J. Xu¹, L. Xu¹, Q. J. Xu¹³, X. P. Xu³⁷, L. Yan^{49A,49C}, W. B. Yan^{46,a}, W. C. Yan^{46,a}, Y. H. Yan¹⁸, H. J. Yang³⁴, H. X. Yang¹, L. Yang⁵¹, Y. Yang⁶, Y. X. Yang¹¹, M. Ye^{1,a}, M. H. Ye⁷, J. H. Yin¹, B. X. Yu^{1,a}, C. X. Yu³⁰, J. S. Yu²⁶, C. Z. Yuan¹, W. L. Yuan²⁹, Y. Yuan¹, A. Yuncu^{40B,c}, A. A. Zafar⁴⁸, A. Zallo^{20A}, Y. Zeng¹⁸, Z. Zeng^{46,a}, B. X. Zhang¹, B. Y. Zhang^{1,a}, C. Zhang²⁹, C. C. Zhang¹, D. H. Zhang¹, H. H. Zhang³⁸, H. Y. Zhang^{1,a}, J. Zhang¹, J. J. Zhang¹, J. L. Zhang¹, J. Q. Zhang¹, J. W. Zhang^{1,a}, J. Y. Zhang¹, J. Z. Zhang¹, K. Zhang¹, L. Zhang¹, X. Y. Zhang³³, Y. Zhang¹, Y. N. Zhang⁴¹, Y. H. Zhang^{1,a}, Y. T. Zhang^{46,a}, Yu Zhang⁴¹, Z. H. Zhang⁶, Z. P. Zhang⁴⁶, Z. Y. Zhang⁵¹, G. Zhao¹, J. W. Zhao^{1,a}, J. Y. Zhao¹, J. Z. Zhao^{1,a}, Lei Zhao^{46,a}, Ling Zhao¹, M. G. Zhao³⁰, Q. Zhao¹, Q. W. Zhao¹, S. J. Zhao⁵³, T. C. Zhao¹, Y. B. Zhao^{1,a}, Z. G. Zhao^{46,a}, A. Zhemchugov^{23,d}, B. Zheng⁴⁷, J. P. Zheng^{1,a}, W. J. Zheng³³, Y. H. Zheng⁴¹, B. Zhong²⁸, L. Zhou^{1,a}, X. Zhou⁵¹, X. K. Zhou^{46,a}, X. R. Zhou^{46,a}, X. Y. Zhou¹, K. Zhu¹, K. J. Zhu^{1,a}, S. Zhu¹, S. H. Zhu⁴⁵, X. L. Zhu³⁹, Y. C. Zhu^{46,a}, Y. S. Zhu¹, Z. A. Zhu¹, J. Zhuang^{1,a}, L. Zotti^{49A,49C}, B. S. Zou¹, J. H. Zou¹

(BESIII Collaboration)

¹ Institute of High Energy Physics, Beijing 100049, People's Republic of China² Beihang University, Beijing 100191, People's Republic of China³ Beijing Institute of Petrochemical Technology, Beijing 102617, People's Republic of China⁴ Bochum Ruhr-University, D-44780 Bochum, Germany⁵ Carnegie Mellon University, Pittsburgh, Pennsylvania 15213, USA⁶ Central China Normal University, Wuhan 430079, People's Republic of China⁷ China Center of Advanced Science and Technology, Beijing 100190, People's Republic of China⁸ COMSATS Institute of Information Technology, Lahore, Defence Road, Off Raiwind Road, 54000 Lahore, Pakistan⁹ G.I. Budker Institute of Nuclear Physics SB RAS (BINP), Novosibirsk 630090, Russia¹⁰ GSI Helmholtzcentre for Heavy Ion Research GmbH, D-64291 Darmstadt, Germany

- ¹¹ Guangxi Normal University, Guilin 541004, People's Republic of China
¹² GuangXi University, Nanning 530004, People's Republic of China
¹³ Hangzhou Normal University, Hangzhou 310036, People's Republic of China
¹⁴ Helmholtz Institute Mainz, Johann-Joachim-Becher-Weg 45, D-55099 Mainz, Germany
¹⁵ Henan Normal University, Xinxiang 453007, People's Republic of China
¹⁶ Henan University of Science and Technology, Luoyang 471003, People's Republic of China
¹⁷ Huangshan College, Huangshan 245000, People's Republic of China
¹⁸ Hunan University, Changsha 410082, People's Republic of China
¹⁹ Indiana University, Bloomington, Indiana 47405, USA
²⁰ (A)INFN Laboratori Nazionali di Frascati, I-00044, Frascati, Italy; (B)INFN and University of Perugia, I-06100, Perugia, Italy
²¹ (A)INFN Sezione di Ferrara, I-44122, Ferrara, Italy; (B)University of Ferrara, I-44122, Ferrara, Italy
²² Johannes Gutenberg University of Mainz, Johann-Joachim-Becher-Weg 45, D-55099 Mainz, Germany
²³ Joint Institute for Nuclear Research, 141980 Dubna, Moscow region, Russia
²⁴ Justus Liebig University Giessen, II. Physikalisches Institut, Heinrich-Buff-Ring 16, D-35392 Giessen, Germany
²⁵ KVI-CART, University of Groningen, NL-9747 AA Groningen, The Netherlands
²⁶ Lanzhou University, Lanzhou 730000, People's Republic of China
²⁷ Liaoning University, Shenyang 110036, People's Republic of China
²⁸ Nanjing Normal University, Nanjing 210023, People's Republic of China
²⁹ Nanjing University, Nanjing 210093, People's Republic of China
³⁰ Nankai University, Tianjin 300071, People's Republic of China
³¹ Peking University, Beijing 100871, People's Republic of China
³² Seoul National University, Seoul, 151-747 Korea
³³ Shandong University, Jinan 250100, People's Republic of China
³⁴ Shanghai Jiao Tong University, Shanghai 200240, People's Republic of China
³⁵ Shanxi University, Taiyuan 030006, People's Republic of China
³⁶ Sichuan University, Chengdu 610064, People's Republic of China
³⁷ Soochow University, Suzhou 215006, People's Republic of China
³⁸ Sun Yat-Sen University, Guangzhou 510275, People's Republic of China
³⁹ Tsinghua University, Beijing 100084, People's Republic of China
⁴⁰ (A)Istanbul Aydin University, 34295 Sefakoy, Istanbul, Turkey; (B)Istanbul Bilgi University, 34060 Eyup, Istanbul, Turkey; (C)Uludag University, 16059 Bursa, Turkey
⁴¹ University of Chinese Academy of Sciences, Beijing 100049, People's Republic of China
⁴² University of Hawaii, Honolulu, Hawaii 96822, USA
⁴³ University of Minnesota, Minneapolis, Minnesota 55455, USA
⁴⁴ University of Rochester, Rochester, New York 14627, USA
⁴⁵ University of Science and Technology Liaoning, Anshan 114051, People's Republic of China
⁴⁶ University of Science and Technology of China, Hefei 230026, People's Republic of China
⁴⁷ University of South China, Hengyang 421001, People's Republic of China
⁴⁸ University of the Punjab, Lahore-54590, Pakistan
⁴⁹ (A)University of Turin, I-10125, Turin, Italy; (B)University of Eastern Piedmont, I-15121, Alessandria, Italy; (C)INFN, I-10125, Turin, Italy
⁵⁰ Uppsala University, Box 516, SE-75120 Uppsala, Sweden
⁵¹ Wuhan University, Wuhan 430072, People's Republic of China
⁵² Zhejiang University, Hangzhou 310027, People's Republic of China
⁵³ Zhengzhou University, Zhengzhou 450001, People's Republic of China
^a Also at State Key Laboratory of Particle Detection and Electronics, Beijing 100049, Hefei 230026, People's Republic of China
^b Also at Ankara University, 06100 Tandogan, Ankara, Turkey
^c Also at Bogazici University, 34342 Istanbul, Turkey
^d Also at the Moscow Institute of Physics and Technology, Moscow 141700, Russia
^e Also at the Functional Electronics Laboratory, Tomsk State University, Tomsk, 634050, Russia
^f Also at the Novosibirsk State University, Novosibirsk, 630090, Russia
^g Also at the NRC "Kurchatov" Institute, PNPI, 188300, Gatchina, Russia
^h Also at University of Texas at Dallas, Richardson, Texas 75083, USA
ⁱ Also at Istanbul Arel University, 34295 Istanbul, Turkey

A neutral structure in the $D\bar{D}^*$ system around the $D\bar{D}^*$ mass threshold is observed with a statistical significance greater than 10σ in the processes $e^+e^- \rightarrow D^+D^{*-}\pi^0 + c.c.$ and $e^+e^- \rightarrow D^0\bar{D}^{*0}\pi^0 + c.c.$ at $\sqrt{s} = 4.226$ and 4.257 GeV in the BESIII experiment. The structure is denoted as $Z_c(3885)^0$. Assuming the presence of a resonance, its pole mass and width are determined to be $(3885.7_{-5.7}^{+4.3}(\text{stat}) \pm 8.4(\text{syst}))$ MeV/ c^2 and $(35_{-12}^{+11}(\text{stat}) \pm 15(\text{syst}))$ MeV, respectively. The Born cross sections are measured to be $\sigma(e^+e^- \rightarrow Z_c(3885)^0\pi^0, Z_c(3885)^0 \rightarrow D\bar{D}^*) = (77 \pm 13(\text{stat}) \pm 17(\text{syst}))$ pb at 4.226 GeV and $(47 \pm 9(\text{stat}) \pm 10(\text{syst}))$ pb at 4.257 GeV. The ratio of decay rates $\frac{\mathcal{B}(Z_c(3885)^0 \rightarrow D^+D^{*-} + c.c.)}{\mathcal{B}(Z_c(3885)^0 \rightarrow D^0\bar{D}^{*0} + c.c.)}$ is determined to be $0.96 \pm 0.18(\text{stat}) \pm 0.12(\text{syst})$, consistent with no isospin violation in the process $Z_c(3885)^0 \rightarrow D\bar{D}^*$.

PACS numbers: 14.40.Rt, 13.25.Gv, 13.66.Bc

The existence of exotic states beyond those of conventional mesons and baryons was debated for decades, mostly because no convincing experimental evidence for them had been found [1]. In recent years, the discovery of charged Z_c charmonium-like states [2, 3], which decay to a charmonium state plus a pion or a pair of charmed mesons and, therefore, must consist of at least a four constituent quark configuration $c\bar{c}q\bar{q}'$, has stirred excitement about these possible exotic states. In $e^+e^- \rightarrow \pi^\mp Z_c^\pm$ processes, four Z_c^\pm states have been discovered in the decays of $Z_c(3885)^\pm \rightarrow (D\bar{D}^*)^\pm$ [4, 5], $Z_c(3900)^\pm \rightarrow \pi^\pm J/\psi$ [6–8], $Z_c(4020)^\pm \rightarrow \pi^\pm h_c$ [9], and $Z_c(4025)^\pm \rightarrow (D^*\bar{D}^*)^\pm$ [10]. There have been many theoretical predictions and interpretations [3] to explain their nature as exotic mesons. However, none of these models have either been ruled out or established experimentally.

After the discoveries of the charged Z_c^\pm states, BESIII reported studies of their neutral partners in the isospin symmetric channel of $e^+e^- \rightarrow \pi^0 Z_c^0$. A $Z_c(3900)^0$ is found in $e^+e^- \rightarrow \pi^0\pi^0 J/\psi$ [11], a $Z_c(4020)^0$ in $e^+e^- \rightarrow \pi^0\pi^0 h_c$ [12], and a $Z_c(4025)^0$ in $e^+e^- \rightarrow \pi^0(D^*\bar{D}^*)^0$ [13]. Evidence for $Z_c(3900)^0$ in $e^+e^- \rightarrow \pi^0 Z_c^0$ was previously reported with CLEO-c data at $\sqrt{s} = 4.17$ GeV [8]. These measurements indicate that the $Z_c(3900)$, $Z_c(4020)$ and $Z_c(4025)$ are three different isospin triplet states, since their relative Born cross sections of the charged modes to the neutral modes are compatible with isospin conservation. This motivates a search for the neutral partner of the $Z_c(3885)^\pm$ in $e^+e^- \rightarrow (D\bar{D}^*)^0\pi^0 + c.c.$ to identify its isospin.

In this Letter, the process $e^+e^- \rightarrow (D\bar{D}^*)^0\pi^0 + c.c.$ is studied, where $(D\bar{D}^*)^0$ refers to D^+D^{*-} or $D^0\bar{D}^{*0}$. A neutral charmonium-like structure, the $Z_c(3885)^0$, is observed around the $(D\bar{D}^*)^0$ mass threshold in the $(D\bar{D}^*)^0$ mass spectrum. This analysis is based on data samples collected by the BESIII detector with integrated luminosities of 1092 pb^{-1} at $\sqrt{s} = 4.226$ GeV and 826 pb^{-1} at $\sqrt{s} = 4.257$ GeV [14, 15]. Note that charge conjugation is always implied, unless explicitly stated.

BESIII [16] is a general-purpose detector at the double-ring e^+e^- collider BEPCII, which is used for the study of physics in the τ -charm energy region [17]. Monte Carlo (MC) simulations based on GEANT4 [18] are

implemented in the BESIII experiment. For each energy point, we generate a signal MC sample based on the covariant tensor amplitude formalism [19] to simulate the S -wave process $e^+e^- \rightarrow Z_c^0\pi^0 \rightarrow (D\bar{D}^*)^0\pi^0$, assuming that the Z_c^0 has $J^P = 1^+$. Effects of initial state radiation are taken into account with the MC event generator KKMC [20, 21], where the line shape of the Born cross section of $e^+e^- \rightarrow Z_c^0\pi^0 \rightarrow (D\bar{D}^*)^0\pi^0$ is assumed to follow that of the charged channel $e^+e^- \rightarrow Z_c^\pm\pi^\mp \rightarrow (D\bar{D}^*)^\pm\pi^\mp$ [4]. In addition, a large statistics MC sample of the three body process $e^+e^- \rightarrow (D\bar{D}^*)^0\pi^0$ is generated according to phase space (PHSP). To study possible backgrounds, MC simulations of $Y(4260)$ generic decays, initial state radiation production of the vector charmonium states, charmed meson production, and the continuum process $e^+e^- \rightarrow q\bar{q}$ ($q = u, d, s$) equivalent to 10 times the luminosity of the data at $\sqrt{s} = 4.226$ and 4.257 GeV are generated. Particle decays are simulated with EVTGEN [22, 23] for the known decay modes with branching fractions set to the world average [1] and with the LUNDCHARM model [24] for the remaining unknown decays.

In this work, we study $e^+e^- \rightarrow D^+D^{*-}\pi^0$, $D^{*-} \rightarrow \bar{D}^0\pi^-$ based on the detection of the $D^+\bar{D}^0$ pair and $e^+e^- \rightarrow D^0\bar{D}^{*0}\pi^0$, $\bar{D}^{*0} \rightarrow \bar{D}^0\pi^0$ based on the detection of the $D^0\bar{D}^0$ pair. The $D\bar{D}$ meson pairs are reconstructed through five hadronic decay modes $K^-\pi^+\pi^+$, $K^-\pi^+\pi^+\pi^0$, $K_S\pi^+$, $K_S\pi^+\pi^0$, $K_S\pi^+\pi^+\pi^-$ for the D^+ and three modes $K^+\pi^-$, $K^+\pi^-\pi^0$, $K^+\pi^+\pi^+\pi^-$ for the \bar{D}^0 . The primary π^0 , which is produced along with the $D\bar{D}^*$ in the e^+e^- reaction, is reconstructed from a pair of photons, while the soft π from the D^* decay is not required to improve the detection efficiency. The D^+D^- mode is not included because of its low rate compared to $D^0\bar{D}^0$ and $D^+\bar{D}^0$.

In this analysis, the selection criteria in Ref. [5] are used to identify the π^\pm/K^\pm , photon, π^0 and K_S candidates. The charged-particle tracks in each D candidate are constrained to a common vertex, except for those from K_S decays, and the χ^2 of the vertex fit is required to be less than 100. Each D candidate is required to have its reconstructed invariant mass in the range $(1.840, 1.880)$ GeV/ c^2 . Furthermore, a mass-constrained kinematic fit (KF) to the nominal D mass is

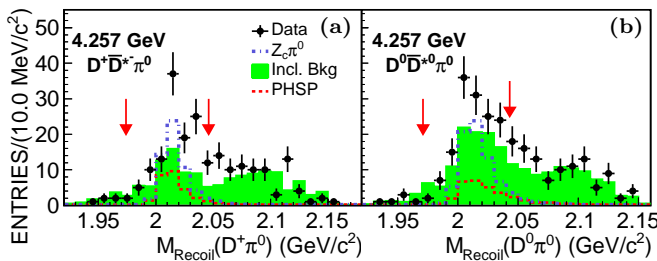


FIG. 1. Distributions of $\text{RM}(D\pi^0)$ at $\sqrt{s} = 4.257$ GeV. The signal and PHSP processes are overlaid with an arbitrary scale. The solid arrows indicate the selection criteria for the $(D\bar{D}^*)^0\pi^0$ candidates. Data at $\sqrt{s} = 4.226$ GeV show similar distributions and are omitted.

performed, and the KF chisquare χ_D^2 is required to be less than 100. In case there is more than one $D\bar{D}$ combination in an event, only the candidate with the minimum sum of $\chi_D^2 + \chi_{\bar{D}}^2$ is kept. The $D\bar{D}$ four-momenta from the mass-constrained KF are used for the further analysis.

The primary π^0 candidates are reconstructed with pairs of photons which are not used in forming the $D\bar{D}$ mesons, and their invariant masses $M(\gamma\gamma)$ must be in the range (0.120, 0.150) GeV/c^2 . To reduce backgrounds and to improve the resolution, a KF with 2 degrees of freedom (2C) is performed, constraining $M(\gamma\gamma)$ to the nominal π^0 mass $m(\pi^0)$ and the recoil mass of $\pi^0 D\bar{D}$, $\text{RM}(\pi^0 D\bar{D})$, to the nominal π mass. The 2C KF chisquare $\chi_{2C}^2(\pi)$ must be less than 200. For each $D\bar{D}$ mode, if there is more than one primary π^0 candidate, the one with the minimum $\chi_{2C}^2(\pi)$ is retained for further analysis. For $e^+e^- \rightarrow D^0\bar{D}^{*0}\pi^0$ with $\bar{D}^{*0} \rightarrow \bar{D}^0\pi^0$, the process $e^+e^- \rightarrow D^0\bar{D}^{*0}\pi^0$ with $\bar{D}^{*0} \rightarrow \bar{D}^0\gamma$ is a major background. To reject this background, we require $\chi_{2C}^2(\pi^0) < 60$. We also perform a similar 2C KF but constrain $\text{RM}(\pi^0 D^0\bar{D}^0)$ to be zero, which corresponds to the mass of the photon in $\bar{D}^{*0} \rightarrow \bar{D}^0\gamma$, and the corresponding fit chisquare is required to satisfy $\chi_{2C}^2(\gamma) > 20$ to further suppress this background. The fitted four-momentum of the primary π^0 is used in the next stage of the analysis.

In the surviving events, the occurrence of multiple $(D\bar{D}^*)^0\pi^0$ combinations per event is negligible. To help separate the signal events, we require $M(D^+\pi^0) > 2.1$ GeV/c^2 and $M(D^0\pi^0) > 2.1$ GeV/c^2 [25]. Because of the limited phase space, the invariant mass of $D^+\pi^0$ ($D^0\pi^0$) and that of $\bar{D}^0\pi^0$ are highly correlated, and the background with the selected π^0 and \bar{D}^0 from the \bar{D}^{*0} decay is suppressed by the above selection criteria, too. The $\text{RM}(D\pi^0)$ distributions are illustrated in Fig. 1, where clear peaks are seen over simulated backgrounds around the $m(D^*)$ position. These peaks correspond to the final states of $(D\bar{D}^*)^0\pi^0$. We further require events to be within the mass window $|\text{RM}(D\pi^0) - m(D^*)| < 36$ MeV/c^2 for the final analysis.

The $M(D\bar{D}^*)$ distribution of the surviving events is plotted in Fig. 2. An enhancement near the $D\bar{D}^*$ mass threshold around 3.9 GeV/c^2 is visible, which is seen in both $D^+D^{*-}\pi^0$ and $D^0\bar{D}^{*0}\pi^0$ at $\sqrt{s} = 4.226$ and 4.257 GeV. As verified in MC simulations, these structures cannot be attributed to the $e^+e^- \rightarrow (D\bar{D}^*)^0\pi^0$ three body PHSP or inclusive MC background. Possible backgrounds from $e^+e^- \rightarrow D^{(*)}\bar{D}^{**} \rightarrow D\bar{D}^*\pi$ have been studied. Most of them, such as $D^*\bar{D}^*(2400)$, $D\bar{D}^*(2460)$ and $D^*\bar{D}^*(2420)$ cannot contribute to the selected events since their mass thresholds are higher than 4.26 GeV/c^2 . The only possible peaking background $e^+e^- \rightarrow D^{(*)}\bar{D}_1(2420)$ has been studied in Ref. [5], and its contribution is found to be negligible.

Assuming that there is a resonant structure close to the $D\bar{D}^*$ mass threshold (labeled as $Z_c(3885)^0$), we model its line shape using a relativistic S -wave Breit-Wigner function with a mass-dependent width multiplied with a phase space factor q

$$\left| \frac{\sqrt{M\Gamma_I(M)/c^2}}{M^2 - m^2 + iM(\Gamma_1(M) + \Gamma_2(M))/c^2} \right|^2 q \quad (I = 1, 2),$$

where $\Gamma_I(M) = \Gamma_I \cdot (m/M) \cdot (p_I^*/p_I^0)$. I denotes the different decay modes, where $I = 1$ represents the D^+D^{*-} decay mode and $I = 2$ represents the $D^0\bar{D}^{*0}$ decay mode. M is the reconstructed mass, m is the nominal resonance mass and Γ_I is the partial width of the decay channel I . Under the assumption of isospin symmetry, we take Γ_I to be half of the full width Γ , assuming that the decay rates to other possible coupled channels are negligible. $p_I^*(q)$ is the momentum of the $D(\pi^0)$ in the rest frame of the $D\bar{D}^*$ system (the initial e^+e^- system), and p_I^0 is the momentum of the D in the resonance rest frame at $M = m$.

An unbinned maximum likelihood fit is performed on the $M(D\bar{D}^*)$ spectra for $e^+e^- \rightarrow (D\bar{D}^*)^0\pi^0$ simultaneously at $\sqrt{s} = 4.226$ and 4.257 GeV. Three components are included in the fits: the $Z_c(3885)^0$ signal, the PHSP processes and MC simulated backgrounds. The signal shape is described as a mass-dependent-efficiency weighted Breit-Wigner function, described above, convoluted with the experimental resolution function. The resolution function and the efficiency shape are obtained from MC simulations. The shape of the PHSP processes is derived from MC simulations, and their amplitudes are allowed to vary in the fits. The inclusive MC background distributions are modeled based on the kernel estimation [26], and their sizes are fixed according to the expected numbers estimated in the inclusive MC samples. The simulated backgrounds are validated by comparing their $M(D\pi^0)$ and $\text{RM}(D\pi^0)$ distributions with those for data in sideband regions (1.920, 1.974) \cup (2.090, 2.180) GeV/c^2 for the $D^+\bar{D}^0$ mode and (1.920, 1.971) \cup (2.090, 2.160) GeV/c^2 for the $D^0\bar{D}^0$ mode.

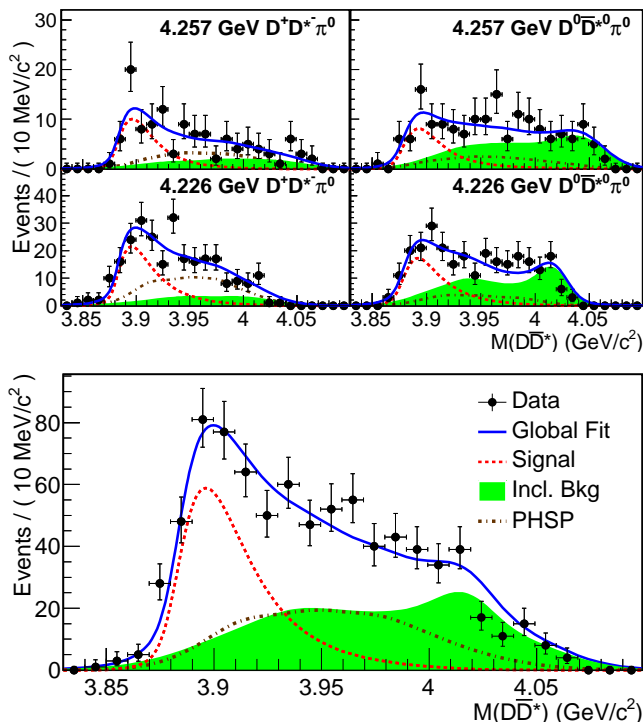


FIG. 2. (Upper) Projections of the simultaneous fit to the $M(D\bar{D}^*)$ spectra for $e^+e^- \rightarrow D^+D^{*-}\pi^0$ and $D^0\bar{D}^{*0}\pi^0$ at $\sqrt{s} = 4.226$ and 4.257 GeV. (Lower) Sum of the simultaneous fit to the $M(D\bar{D}^*)$ spectra for different decay modes at the different energy points above.

We define the ratio $\mathcal{R} = \mathcal{B}_{D^+D^{*-}}/\mathcal{B}_{D^0\bar{D}^{*0}}$, where $\mathcal{B}_{D^+D^{*-}}$ ($\mathcal{B}_{D^0\bar{D}^{*0}}$) is the branching ratio of $Z_c(3885)^0 \rightarrow D^+D^{*-}$ ($D^0\bar{D}^{*0}$). In the fit, \mathcal{R} is assumed to be same for the data at $\sqrt{s} = 4.226$ and 4.257 GeV. The number of observed signal events, N_{obs} , is given by $N_{\text{obs}} = \mathcal{L}\sigma_{D\bar{D}^*}(1+\delta^{\text{rad}})(1+\delta^{\text{vac}})\varepsilon\mathcal{B}_{\text{int}}$, where $\sigma_{D\bar{D}^*}$ is the Born cross section $\sigma(e^+e^- \rightarrow Z_c(3885)^0\pi^0, Z_c(3885)^0 \rightarrow D\bar{D}^*)$, \mathcal{L} is the integrated luminosity, $(1+\delta^{\text{rad}})$ is the initial radiative correction factor, $(1+\delta^{\text{vac}})$ is the vacuum polarization factor [27], ε is the detection efficiency and \mathcal{B}_{int} is the product of the decay rates of the intermediate states.

Figure 2 shows the fit results. To assess the goodness of fit, we bin the data set in 19 bins such that each bin contains at least 10 events, and compute the χ^2 between the binned data and the projection of the fit. We find $\chi^2/\text{d.o.f.} = 18.5/19$ for the simultaneous fit in the lower plot. The statistical significance of the $Z_c(3885)^0$ signal is estimated to be more than 12σ , based on the difference of the maximized likelihoods between the fit with and without including the signal component. The mass and width of the $Z_c(3885)^0$ are measured to be $m(Z_c(3885)^0) = (3894.7 \pm 3.0)$ MeV/ c^2 and $\Gamma(Z_c(3885)^0) = (36 \pm 17)$ MeV. The corresponding pole mass and width are calculated to be $m_{\text{pole}}(Z_c(3885)^0) = 3885.7_{-5.7}^{+4.3}$ MeV/ c^2 and

TABLE I. Summary of systematic uncertainties for the resonance parameters, the Born cross sections and the ratio of decay rates. Values outside the parenthesis represents uncertainties for $\sigma_{D\bar{D}^*}$ at $\sqrt{s} = 4.226$ GeV, while those inside are for $\sigma_{D\bar{D}^*}$ at $\sqrt{s} = 4.257$ GeV. The total systematic uncertainties are obtained by combining all the independent sources in quadrature.

Source	m_{pole} (MeV/ c^2)	Γ_{pole} (MeV)	$\sigma_{D\bar{D}^*}$ (%)	\mathcal{R} (%)
Beam energy	1.0	3.0	4 (5)	1
Signal shape	3.5	8.2	5 (4)	2
Background	6.8	6.6	15 (15)	4
Fit range	0.3	0.3	3 (1)	1
Mass shift	3.0			
Resolution		9.5	11 (4)	1
Efficiency			11 (11)	11
Input-output check ($1+\delta^{\text{rad}}$)($1+\delta^{\text{vac}}$)	1.6	2.5	5 (5)	
\mathcal{B}_{int}			5 (5)	5
\mathcal{L}			1 (1)	
Total	8.4	15	23 (21)	13

$\Gamma_{\text{pole}}(Z_c(3885)^0) = 35_{-12}^{+11}$ MeV [28]. From the fit, we determine $\sigma_{D\bar{D}^*}$ to be (77 ± 13) pb and (47 ± 9) pb at $\sqrt{s} = 4.226$ and 4.257 GeV, respectively. We also obtain $\mathcal{R} = 0.96 \pm 0.18$.

The systematic uncertainties on the measurements of the $Z_c(3885)^0$ resonance parameters, the cross section $\sigma_{D\bar{D}^*}$ and the ratio \mathcal{R} are studied, and the major contributions are summarized in Table I. The systematic uncertainties on the $Z_c(3885)^0$ resonance parameters mainly come from the signal shape, background, mass shift and detector resolution. The dominant systematic uncertainties on $\sigma_{D\bar{D}^*}$ and \mathcal{R} are from the background, resolution and detection efficiency.

The uncertainty from the beam energy is estimated by varying the beam energy by ± 1 MeV in the 2C KF, and the maximum differences of the mass, width, $\sigma_{D\bar{D}^*}$ at $\sqrt{s} = 4.226$ (4.257) GeV and \mathcal{R} are found to be 1.0 MeV/ c^2 , 3.0 MeV, 5%(4%) and 1%, respectively. To assess the uncertainty of the signal shape, an S -wave relativistic Breit-Wigner function with constant width [28] is taken as an alternative signal model in the simultaneous fit. The changes of the fitted mass and width are determined to be 3.5 MeV/ c^2 and 8.2 MeV, while the change on $\sigma_{D\bar{D}^*}$ is 5%(4%) at $\sqrt{s} = 4.226$ (4.257) GeV and on \mathcal{R} 2%. The systematic uncertainty due to the background description is estimated by leaving free the absolute numbers of the inclusive backgrounds in the fit, or adjusting their shapes by varying the scalings of different background components in the inclusive MC samples. Those fit results differ from the nominal results by 6.8 MeV/ c^2 in mass, 6.6 MeV in width, 15% in $\sigma_{D\bar{D}^*}$ both at $\sqrt{s} = 4.226$ and 4.257 GeV, and 4% in \mathcal{R} . Maximum fluctuations due to changing the fit range are assigned as systematic uncertainties. The MC simulation of the mass shift and resolution may not fully reflect the effects in data, and it is studied by fitting the

\bar{D}^* peak in the $\text{RM}(D\pi^0)$ spectra to obtain the mass shift and the resolution difference between data and MC simulations. The obtained mass shift is quoted as part of the systematic uncertainties of the mass. The variations of the fit results after considering the resolution difference is assigned as systematic uncertainty.

Efficiency-related systematic uncertainties are universal in each D decay mode and include six sources: tracking efficiency, particle identification, photon detection efficiency, π^0 reconstruction efficiency, K_S reconstruction efficiency and KF efficiency. The uncertainties of tracking efficiency and particle identification for π^\pm and K^\pm are evaluated to be 1% per track [29, 30]. The uncertainty in the photon-reconstruction efficiency is estimated to be about 1% per photon [31]. The efficiency difference of reconstructing the K_S in MC simulations and in data is 4.0% [32]. The uncertainty in π^0 reconstruction is 1% [31]. The systematic bias of the KF is estimated by using the track-parameter-correction method [33]. The correction factors for helix track parameters are determined from the control sample $e^+e^- \rightarrow K^*(892)^0 K^+\pi^- \rightarrow K^+K^-\pi^+\pi^-$. The total efficiency-related systematic uncertainty is taken as the square root of the quadratic sum of the individual uncertainties. The potential bias from the event selection and the analysis procedure is studied with input-output checks, which compare the output results with the input values of the resonance mass and width based on MC simulations. We assign the systematic uncertainty of 1.6 MeV/ c^2 in mass and 2.5 MeV in width accordingly. The systematic uncertainty of the radiative correction factor $1 + \delta^{\text{rad}}$, which includes the effect on the detection efficiency, is estimated to be 5% by changing the input $(D\bar{D}^*)^0\pi^0$ line shape within errors [4]. The systematic uncertainty of the vacuum polarization factor $1 + \delta^{\text{vac}}$ is 0.5% taken from the QED calculation [27]. The weighted systematic uncertainty of \mathcal{B}_{int} is from the world average value [1]. The uncertainty of integrated luminosity is taken as 1% by measuring Bhabha events [14]. The uncertainty of the mass window requirement is negligible. The overall systematic uncertainties are determined by combining all the sources in quadrature, assuming they are independent.

In summary, we study $e^+e^- \rightarrow D^+D^{*-}\pi^0 + c.c.$ and $e^+e^- \rightarrow D^0\bar{D}^{*0}\pi^0 + c.c.$ using data taken at $\sqrt{s} = 4.226$ and 4.257 GeV. A neutral structure around the $D\bar{D}^*$ mass threshold is observed with a statistical significance greater than 10σ . Assuming that it is a resonance, we model it with a relativistic Breit-Wigner function. Its pole mass and width are measured to be $(3885.7_{-5.7}^{+4.3}(\text{stat}) \pm 8.4(\text{syst}))$ MeV/ c^2 and $(35_{-12}^{+11}(\text{stat}) \pm 15(\text{syst}))$ MeV, respectively, which are close to the mass and width of the reported charged $Z_c(3885)^+$ [4, 5]. The Born cross sections $\sigma(e^+e^- \rightarrow Z_c^0\pi^0 \rightarrow (D\bar{D}^*)^0\pi^0 + c.c.)$ are determined to be $(77 \pm 13 \pm 17)$ pb and $(47 \pm 9 \pm 10)$ pb at $\sqrt{s} = 4.226$

and 4.257 GeV, respectively, which are consistent with half of $\sigma(e^+e^- \rightarrow Z_c^+\pi^- \rightarrow (D\bar{D}^*)^+\pi^- + c.c.)$ [5]. A comparison between the resonance parameters of the $Z_c(3885)^+$ and the $Z_c(3885)^0$ is summarized in the Supplemental Material [25]. All these observations favor the assumption that the $Z_c(3885)^0$ is the neutral isospin partner of the $Z_c(3885)^\pm$, and the $Z_c(3885)^\pm/Z_c(3885)^0$ form an isospin triplet. In addition, we determine the ratio of the decay rate $\mathcal{R} = \frac{\mathcal{B}(Z_c(3885)^0 \rightarrow D^+D^{*-})}{\mathcal{B}(Z_c(3885)^0 \rightarrow D^0D^{*0})} = 0.96 \pm 0.18 \pm 0.12$, which is consistent with unity. Hence, no isospin violation in the process $Z_c(3885)^0 \rightarrow D\bar{D}^*$ is observed.

The BESIII collaboration thanks the staff of BEPCII and the IHEP computing center for their strong support. This work is supported in part by National Key Basic Research Program of China under Contract No. 2015CB856700; National Natural Science Foundation of China (NSFC) under Contracts Nos. 11125525, 11235011, 11322544, 11335008, 11425524; the Chinese Academy of Sciences (CAS) Large-Scale Scientific Facility Program; the CAS Center for Excellence in Particle Physics (CCEPP); the Collaborative Innovation Center for Particles and Interactions (CICPI); Joint Large-Scale Scientific Facility Funds of the NSFC and CAS under Contracts Nos. 11179007, U1232201, U1332201; CAS under Contracts Nos. KJCX2-YW-N29, KJCX2-YW-N45; 100 Talents Program of CAS; National 1000 Talents Program of China; INPAC and Shanghai Key Laboratory for Particle Physics and Cosmology; German Research Foundation DFG under Contract No. Collaborative Research Center CRC-1044; Istituto Nazionale di Fisica Nucleare, Italy; Ministry of Development of Turkey under Contract No. DPT2006K-120470; Russian Foundation for Basic Research under Contract No. 14-07-91152; The Swedish Research Council; U.S. Department of Energy under Contracts Nos. DE-FG02-04ER41291, DE-FG02-05ER41374, de-sc0012069, DESC0010118; U.S. National Science Foundation; University of Groningen (RuG) and the Helmholtzzentrum fuer Schwerionenforschung GmbH (GSI), Darmstadt; WCU Program of National Research Foundation of Korea under Contract No. R32-2008-000-10155-0.

-
- [1] K. A. Olive *et al.* (Particle Data Group), *Chin. Phys. C* **38**, 090001 (2014).
 - [2] G. T. Bodwin, E. Braaten, E. Eichten, S. L. Olsen, T. K. Pedlar and J. Russ, arXiv:1307.7425; X. Liu, *Chin. Sci. Bull.* **59**, 3815 (2014); S. L. Olsen, *Front. Phys.* **10**, 101401 (2015).
 - [3] N. Brambilla *et al.*, *Eur. Phys. J. C* **71**, 1534 (2011).
 - [4] M. Ablikim *et al.* (BESIII Collaboration), *Phys. Rev. Lett.* **112**, 022001 (2014).
 - [5] M. Ablikim *et al.* (BESIII Collaboration), *Phys. Rev. D* **92**, 092006 (2015).

- [6] M. Ablikim *et al.* (BESIII Collaboration), Phys. Rev. Lett. **110**, 252001 (2013).
- [7] Z. Q. Liu *et al.* (Belle Collaboration), Phys. Rev. Lett. **110**, 252002 (2013).
- [8] T. Xiao, S. Dobbs, A. Tomaradze, and K. K. Seth, Phys. Lett. B **727**, 366 (2013).
- [9] M. Ablikim *et al.* (BESIII Collaboration), Phys. Rev. Lett. **111**, 242001 (2013).
- [10] M. Ablikim *et al.* (BESIII Collaboration), Phys. Rev. Lett. **112**, 132001 (2014).
- [11] M. Ablikim *et al.* (BESIII Collaboration), Phys. Rev. Lett. **115**, 112003 (2015).
- [12] M. Ablikim *et al.* (BESIII Collaboration), Phys. Rev. Lett. **113**, 212002 (2014).
- [13] M. Ablikim *et al.* (BESIII Collaboration), Phys. Rev. Lett. **115**, 182002 (2015).
- [14] M. Ablikim *et al.* (BESIII Collaboration), Chin. Phys. C **39**, 093001 (2015).
- [15] M. Ablikim *et al.* (BESIII Collaboration), arXiv:1510.08654.
- [16] M. Ablikim *et al.* (BESIII Collaboration), Nucl. Instrum. Methods Phys. Res., Sect. A **614**, 345 (2010).
- [17] D. M. Asner *et al.*, Int. J. Mod. Phys. A **24**, 499 (2009).
- [18] S. Agostinelli *et al.* (GEANT4 Collaboration), Nucl. Instrum. Methods Phys. Res., Sect. A **506**, 250 (2003).
- [19] B. S. Zou and D. V. Bugg, Eur. Phys. J. A **16**, 537 (2003).
- [20] S. Jadach, B. F. L. Ward, and Z. Was, Comput. Phys. Commun. **130**, 260 (2000).
- [21] S. Jadach, B. F. L. Ward, and Z. Was, Phys. Rev. D **63**, 113009 (2001).
- [22] D. J. Lange, Nucl. Instrum. Methods Phys. Res., Sect. A **462**, 152 (2001).
- [23] R. G. Ping, Chin. Phys. C **32**, 599 (2008).
- [24] J. C. Chen, G. S. Huang, X. R. Qi, D. H. Zhang, and Y. S. Zhu, Phys. Rev. D **62**, 034003 (2000).
- [25] See Supplemental Material at <http://link.aps.org/supplemental/10.1103/PhysRevLett.115.222002> for the figure of $D\pi^0$ mass distribution and the summary table of $Z_c(3885)$.
- [26] K. S. Cranmer, Comput. Phys. Commun. **136**, 198 (2001).
- [27] S. Actis *et al.*, Eur. Phys. J. C **66**, 585 (2010).
- [28] A. R. Bohm and Y. Sato, Phys. Rev. D **71**, 085018 (2005).
- [29] M. Ablikim *et al.* (BESIII Collaboration), Phys. Rev. Lett. **107**, 092001 (2011).
- [30] M. Ablikim *et al.* (BESIII Collaboration), Phys. Rev. D **83**, 112005 (2011).
- [31] M. Ablikim *et al.* (BESIII Collaboration), Phys. Rev. D **81**, 052005 (2010).
- [32] M. Ablikim *et al.* (BESIII Collaboration), Phys. Rev. D **87**, 052005 (2013).
- [33] M. Ablikim *et al.* (BESIII Collaboration), Phys. Rev. D **87**, 012002 (2013).